Published in final edited form as:
IEEE Trans Biomed Eng. 2008 December ; 55(12): 2691–2700. doi:10.1109/TBME.2008.919132.

Physiologically Based Pharmacokinetic (PBPK) Models for Ethanol

Martin H. Plawecki [Student Member, IEEE], **Jae-Joon Han [Student Member, IEEE]**, **Peter C. Doerschuk*** **[Senior Member, IEEE]**, **Vijay A. Ramchandani**, and **Sean J. O'Connor**

Abstract

Physiologically based pharmacokinetic models have been used to describe the distribution and elimination of ethanol after intravenous administration. These models have been used to estimate the ethanol infusion profile that is sufficient for achieving a prescribed breath ethanol concentration time course in individuals, providing a useful platform for several pharmacokinetic and pharmacodynamic investigations. Mathematical foundations of these models are examined, including the derivation of an explicit set of governing equations in the form of a system of nonlinear ordinary differential equations. These equations can then be used to formulate and refine parameter identification and control strategies. Finally, a framework in which models related to this model can be constructed and analyzed is described.

Keywords

Alcohol; ethanol; model; pharmacokinetics; physiologically based pharmacokinetic (PBPK) models; physiology

I. INTRODUCTION

Mathematical models relating ethanol input and consequent time courses of ethanol in various tissues play an important role in research on the brain's response to ethanol, and such models are reviewed in Section II. This section reviews the goals and practical constraints on such research, and the contribution of this paper.

Ethanol is a naturally produced drug used by humans for thousands of years because of its psychoactive properties. Beneficial when used in moderation [1], excessive use of ethanol can be devastating. Of people who use ethanol, nearly 8% will become addicted during the course of their life, and about a third of them will die of complications attributable to the addiction [2], [3].

*(pd83@cornell.edu)..
M. H. Plawecki is with Indiana University School of Medicine, Indianapolis, IN 46202-5121 USA.
J.-J. Han is with Samsung Advanced Institute of Technology, Yongin-si Gyunggi-do 446-712, South Korea.
P. C. Doerschuk was with the School of Electrical and Computer Engineer ing, Purdue University, West Lafayette, IN 47907 USA. He is now with the Department of Biomedical Engineering and the School of Electrical and Computer Engineering, Cornell University, Ithaca, NY 14853-5401 USA
V. A. Ramchandani was with the Department of Medicine, Indiana University School of Medicine, Indianapolis, IN 46202-5121 USA. He is now with the National Institute on Alcohol Abuse and Alcoholism, National Institute of Health, Bethesda, MD 20892-9304 USA.
S. J. O'Connor is with the Department of Psychiatry, Indiana University School of Medicine, Indianapolis, IN 46202-5121 USA, and also with the Department of Biomedical Engineering, Purdue University, West Lafayette, IN 47907 USA.

[4]In keeping with the bulk of ethanol pharmacokinetic research, we use units of minutes (min) for time, liters (L) or deciliters (dL) for volume, centimeters (cm) for distance, and milligrams (mg) or kilograms (kg) for mass.

In order to detect the differences in the subjective and objective effects of ethanol on human brains that lead to addiction, it is important to be able to expose the brain of each individual human subject to the same time course of ethanol concentration.[1] Achieving the same time course of brain exposure across subjects is a challenging problem for several reasons, starting with the constraint that ethanol cannot be delivered directly to the brain in humans. When the usual route of ethanol administration, oral ingestion, is used, substantial and uncontrollable variation in ethanol absorption kinetics make it impossible to prescribe the time course of brain exposure, even within a factor of two at any moment, reliably [6], [7]. Fortunately, intravenous administration of ethanol entirely circumvents absorption kinetics. Even when administered intravenously, it is difficult to control the time course in more than one organ at a time because ethanol is a tiny polar molecule which is highly soluble in water and barely soluble in fat [8], [9]. Thus, for a fixed infusion profile, the time course of ethanol exposure in any organ varies considerably from subject to subject due to variability in body size and composition of the subjects in addition to metabolic and circulatory parameters. Even when the goal is to control the exposure in only one organ, the brain, a model of an individual's ethanol kinetics is required before the idiosyncratic infusion profiles that yield the same brain exposure in all subjects can be achieved.

In order to achieve control of brain ethanol exposure, it would be useful to measure brain ethanol concentration directly and frequently, but that measurement is impossible in humans. Fortunately, the brain is a high blood-flow, small water-volume organ, and ethanol readily crosses the blood-brain barrier. Thus, the brain concentration of ethanol follows the arterial ethanol concentration closely, an assumption supported by animal studies [10], [11]. Therefore, breath alcohol concentration (BrAC) is commonly used as a surrogate for brain concentration (please see [12]–[16] for examples), because a correctly performed breath test on end-expiratory air gives a reasonable approximation to arterial ethanol concentration that is the same throughout the body, and because accurate measurements of BrAC are easily achieved in cooperative subjects [17]. In the quest for experimental control of brain exposure to ethanol in human studies, such measurements help validate the models used to compensate for the differences in individual pharmacokinetics.

This paper studies one prominent Physiologically based pharmacokinetic (PBPK) model [6], [7], [12]–[14], [18]–[30] developed at the Indiana Alcohol Research Center (IARC) of the Indiana University School of Medicine. The IARC model, designated PBPK2, was developed in order to control the brain exposure to ethanol of an individual human subject resulting from a controlled intravenous ethanol dose time course through the modeling of the subject's specific ethanol pharmacokinetics of ethanol distribution and elimination. By prescribing the same brain exposure in all subjects, a stable background upon which comparative pharmacodynamic studies of genetic contributions to variable ethanol pharmacokinetic effects can be performed is achieved. The focus on an individual restricted the complexity of the model because it must be possible to determine most, if not all, of the parameter values from practical tests on an individual human subject.

The remainder of the paper is organized as follows. Section II describes selected prior work on ethanol pharmacokinetics focusing on work related to the Physiologically based approach. Section III presents a graphical method for describing the PBPK2 model and related models that is analogous to a circuit diagram except that there are two “charges” flowing in the circuit, blood and ethanol. Section IV describes the PBPK3 model, which contains an additional state variable relative to the PBPK2 model, the concentration of ethanol in the liver, and an additional parameter, the liver volume. Section V describes the PBPK2 model as an approximation to the PBPK3 model that removes the requirement in the PBPK3 model that the liver volume be specified. However, it is still necessary to compute a liver ethanol concentration because that concentration controls the metabolism of ethanol.

The result of using a concentration definition that is not a state variable is anomalous behavior at low ethanol concentrations: the mass flow of ethanol being metabolized by the liver can be greater than the total mass flow to the organ. Section VI describes an example based on intravenous infusion of ethanol in a human volunteer that contrasts the PBPK2 and PBPK3 models. Finally, the paper ends with a discussion in Section VII. While the PBPK2 model was developed as a Simulink[2] program, both the PBPK2 and PBPK3 models are derived here as systems of nonlinear ordinary differential equations that allow a large variety of modern system identification, filtering, and control system design methodologies to be used on these models. In addition to correcting the anomalous behavior of the PBPK2 model, the PBPK3 model is more physiologic. More importantly, it allows for future study of ethanol concentrations in the liver, which can be substantially higher than in other organs because of first-pass exposure to orally ingested ethanol, as well as oral challenge BrAC modeling and experimentation.

II. Ethanol Pharmacokinetic Modeling

Pharmacokinetic modeling for ethanol began in the 1930s with Widmark [31], and continues today in predominantly two forms: phenomenological and physiological. Phenomenological models describe the time series of ethanol concentration in terms of generic compartments where the number of compartments is the order of the linear dynamical system (i.e., the number of time constants) required to fit the time series, e.g., [32]. Physiological models describe the distribution of ethanol in the body in terms of compartments based upon anatomical structures (e.g., a liver compartment) and physiological principles (e.g., conservation of mass), e.g., [32]. Substantial differences exist between the applications to which various models are used. Some models are used to elicit information about large groups of subjects, both human and animal, or populations [11], [33]–[35]. In contrast, other models, such as the PBPK2 model, are models for unique study participants and seek to identify and utilize intersubject variability for possible later study in relationship to the behavior of larger groups [6], [7], [12]–[14], [18]–[22], [24], [27], [29], [30].

Ethanol is distributed by the vascular system and diffuses to and from tissues across the capillary bed. For most of the body, the blood leaving the heart passes through only one capillary bed before returning. However, much of the blood supplied to the gut is collected in the portal venous system, which then supplies the liver, before returning to the heart. Thus, the liver receives both an arterial supply, the hepatic artery, and a venous supply originating from the digestive system, the portal vein. A dual blood supply for the liver is natural since its main function is the metabolic processing of absorbed nutrients, and this dual vascular system provides the physiological basis for the phenomenon of first-pass metabolism of many compounds, including ethanol. Most Physiologically based models of ethanol kinetics contain one or more compartments, representing functional anatomic areas including the portal venous system, and therefore, attempt to describe intravenous and/or oral administration of ethanol. Depending upon the model, each compartment may use separate distribution and elimination kinetics. In contrast, nonphysiologic models lump many or all of these compartments and may only attempt to describe the net elimination of ethanol.

The elimination of ethanol occurs via enzyme systems that obey Michaelis–Menten (MM) kinetics [36]. The MM equation, which is

[1]The pharmacokinetics of ethanol reflects the relationship between the dosing of the drug and the resultant concentration within the body, e.g., the effects of the body upon the drug. The pharmacodynamics reflects the relationship between drug concentration and pharmacologic effect upon tissue, e.g., the effects of the drug upon the body [4, pp. 2566–2574], [5].

$$\frac{dC}{dt} = \frac{V_{\max} C(t)}{k_m + C(t)}, \quad (1)$$

describes the rate of change of concentration [$C(t)$, [mass]/[volume]] of a particular compound due to the action of an enzyme system, where $V_{\max}$ ([concentration]/[time]) is the maximal metabolism rate, and k_m ([concentration]) is the MM constant or concentration of the drug at which metabolism is one-half the maximal rate [37, pp. 192–194]. As the volume of distribution of ethanol is thought to be the entire total body water space [36], distribution kinetics is usually described as a diffusion process, where the rate of change of concentration is proportional to the concentration gradient between compartments [38, pp. 48–49], [39].

Table I describes 17 selected mathematical models for ethanol pharmacokinetics. Many of these particular models share several characteristics; they include MM elimination kinetics, they assume distribution into the entire total body water (TBW) space, and they were used to explain previously recorded BrAC data.

Based upon the animal work of Rheingold *et al.* [40], O'Connor, Ramchandani, and colleagues developed and adapted a three-compartment PBPK model [19], where distribution kinetics are based in part on physiologically relevant cardiac outflow apportionment. This model is similar in many ways to those described in Table I, but the motivation for its development was unique. Specifically, the motivation was experimental control of the time course of brain exposure in individual subjects; only later was the model adapted to animal studies. The novel application was to use the model as part of a system to prescribe an arterial ethanol concentration trajectory, thus a BrAC time course, which is identical for all subjects by determining an appropriate ethanol infusion profile for each. Face validity of their PBPK model was demonstrated by achieving a prescribed, nonnaturally occurring designed BrAC profile across subjects. The initially chosen waveform was a linear rise to a target concentration in a specified time period, the maintenance of that concentration for a specified interval, and a measured, but uncontrolled elimination phase. This process and resulting BrAC waveform is termed the “Indiana alcohol clamp” [19]. The minimization of the pharmacokinetic variability between subjects has allowed for varied pharmacokinetic and pharmacodynamic research, including [6], [7], [12]–[14], and [18]–[30].

III. Model Formulation

Only models that are interconnections of so-called “well-stirred” compartments are to be considered; so, when ethanol enters a compartment, it is assumed that it is instantly spread uniformly and there is a single ethanol concentration for each compartment. The most complicated model to be considered has three compartments that approximate the vasculature, liver, and all other tissues denoted by periphery. It is easier to describe the three-state PBPK3 model first and then present the two-state PBPK2 model, rather than the reverse. Each compartment is described by giving the mass of ethanol in the compartment, and the mathematical model for a compartment is a first-order nonlinear differential equation that describes the time rate of change of the mass of ethanol in the compartment. The interconnections between compartments transport ethanol and blood. The interconnections mimic vascular anatomy and physiology, and include structures such as the portal and hepatic veins. The flux of ethanol into and out of a compartment depends upon the concentration difference.

The vasculature and periphery compartments are similar to the previously described models. The vasculature compartment circulates ethanol through the system at physiologically

relevant concentrations until elimination has been completed. The periphery compartment acts as a storage reservoir from which ethanol may enter or leave, based upon the gradients between its concentration and the arterial and venous ethanol concentrations, respectively.

Ethanol enters the system through two pathways. The simpler pathway is by venous infusion, which occurs only in a laboratory setting. In this case, the mass flow rate of ethanol is added directly to the well-stirred vascular compartment. The more complicated pathway is by oral intake. In this case, the ethanol is transported through the proximal gut and is absorbed in the small intestine from which it enters the portal vein.

PBPK2 model elimination of ethanol occurs only in the liver compartment, and emulates a single enzyme system that follows MM kinetics. In fact, three enzyme systems make up the major ethanol elimination pathways within the liver. The most dominant is alcohol dehydrogenase (ADH), but there are also the microsomal ethanol-oxidizing system and aldehyde dehydrogenase [41]. However, *in vivo* determination of their individual characteristics is impossible and, for that reason, they are lumped into one pathway in this model. Furthermore, other ADH isoforms exist outside of the liver and contribute to elimination from nonliver compartments. However, in any situation where the liver ethanol concentration is roughly the same as the concentration outside of the liver, the greater density of elimination enzymes in the liver means that elimination from the other compartments is considered negligible, a statement supported by animal studies that have shown that 90% of ethanol metabolism occurs within the liver [42].

An important part of the model is the transport of ethanol from the vasculature into and out of the liver and periphery compartments. The flow is driven by the concentration differences. The flow is passive, i.e., it is not coupled to an energy consuming process, and not facilitated, i.e., there is no transporter protein present in only a limited number of copies that lowers the thermodynamic barrier to flow. In order to describe the mathematical model, it is helpful to focus on a specific situation. Therefore, consider the liver, the hepatic artery, the portal vein, which brings material absorbed by the gut to the liver, and the hepatic vein, which connects the liver to the general venous system. Let the ethanol concentrations in the four structures be denoted by $C_{\mathscr{L}}$, C_{HA}, C_{PV}, and C_{HV}, respectively, where the units are [mass]/[volume]. Let the flow rates in the hepatic artery, the portal vein, and the hepatic vein be denoted by R_{HA}, R_{PV}, and R_{HV}, respectively, where the units are [volume]/[time]. The portal vein delivers $C_{\mathrm{PV}}R_{\mathrm{PV}}$ [mass]/[time] of ethanol for potential transport into the liver cells. However, since the transport is down the ethanol concentration gradient, at most $(C_{\mathrm{PV}} - C_{\mathscr{L}})$ [mass]/[time] of ethanol is available for transport since transport of more than this amount would reduce the ethanol concentration in the portal vein below the ethanol concentration in the liver. The remaining ethanol and all of the blood flows through the liver capillary structure and ends up in the hepatic vein. The expression $(C_{\mathrm{PV}} - C_{\mathscr{L}})R_{\mathrm{PV}}$ could be positive or negative. A positive value implies transport into the liver cells from the portal vein, which is the physiological characteristic that it is desired to model. A negative value implies transport out of the liver cells into the portal vein, which is not physiological. In particular, when the ethanol concentration in the liver cells is high and transport down the concentration gradient is out of the liver cells, the destination of the transport is the hepatic vein, not the portal vein. Therefore, for transport from the portal vein into the liver cells, $(C_{\mathrm{PV}} - C_{\mathscr{L}})R_{\mathrm{PV}}$ is replaced by $r(C_{\mathrm{PV}} - C_{\mathscr{L}})R_{\mathrm{PV}}$, where $r(\cdot)$ is the unit ramp defined by $r(x) = xu(x)$ and $u(\cdot)$ is the unit step function. A similar expression can be derived for the transport from the hepatic artery to the liver. The transport of ethanol out of the liver cells will be accounted for by a term $r(C_{\mathscr{L}} - C_{\mathrm{HV}})R_{\mathrm{HV}}$ describing transport out of the liver cells into the hepatic vein. Finally, not all ethanol available for transport need be transported. Therefore, there are dimensionless constants denoted by $k_{\mathrm{PV},\mathscr{L}}$, $k_{\mathrm{HA},\mathscr{L}}$, and $k_{\mathscr{L},\mathrm{HV}}$ that satisfy

$0 \le k_{\mathrm{PV},\mathscr{L}} \le 1$, $0 \le k_{\mathrm{HA},\mathscr{L}} \le 1$, and $0 \le k_{\mathscr{L},\mathrm{HV}} \le 1$ and these constants describe what fraction of the available ethanol is actually transported. The final equations for transport into and out of the liver parenchyma, denoted by $M_{\mathrm{PV},\mathscr{L}}$, $M_{\mathrm{HA},\mathscr{L}}$, and $M_{\mathscr{L},\mathrm{HV}}$, respectively, with units of [mass]/[time] are $M_{\mathrm{PV},\mathscr{L}} = k_{\mathrm{PV},\mathscr{L}}\, r\left(C_{\mathrm{PV}} - C_{\mathscr{L}}\right) R_{\mathrm{PV}}$, $M_{\mathrm{HA},\mathscr{L}} = k_{\mathrm{HA},\mathscr{L}}\, r\left(C_{\mathrm{HA}} - C_{\mathscr{L}}\right) R_{\mathrm{HA}}$ and $M_{\mathscr{L},\mathrm{HV}} = k_{\mathscr{L},\mathrm{HV}}\, r\left(C_{\mathscr{L}} - C_{\mathrm{HV}}\right) R_{\mathrm{HV}}$. Based on this type of example, the generic description of the ethanol transport into the liver or the periphery is

$$M_{x,y}(t) = k_{x,y} R_x\, r\left(C_y(t) - C_x(t)\right) \tag{2}$$

and out of the liver or the periphery is

$$M_{x,y}(t) = k_{x,y} R_y\, r\left(C_y(t) - C_x(t)\right) \tag{3}$$

where $M_{x,y}(t)$ [mass]/[time] is the mass flux of ethanol from x to y at time t; $0 \le k_{x,y} \le 1$ is a dimensionless constant, R_x [volume]/[time] is the volume flow of blood in x, and $C_x(t)$ and $C_y(t)$ [mass]/[volume] are the concentrations of ethanol in x and y, respectively. Equations (2) and (3) have similarities with standard equations for transport across membranes, e.g., [39, Sec. 3.6]. However, the physiological situation here is somewhat different than that in the standard model of membrane transport. For instance, here there are no infinite reservoirs of ethanol but rather ethanol is delivered for potential transport at a fixed rate, and any ethanol that is not transported flows on to a different part of the vasculature. These differences lead to the presence of the unit ramp functions [$r(\cdot)$] and bounds on the dimensionless constants $k_{x,y}$ [$0 \le k_{x,y} \le 1$].

The models described in this paper are roughly similar to electrical circuits, and a graphical description similar to a circuit diagram is useful in understanding what is and what is not included in the model. Such a circuit diagram for a three-compartment model is shown in Fig. 1, where the block diagram fragments labeled A' and B' are to be ignored.

Each compartment in the block diagram of Fig. 1 is labeled with its name, its volume (V_χ variable), and its state variable [$\mu_\chi(t)$ variable], which is the mass of ethanol in the compartment. In addition, $C_\chi(t) \doteq \mu_\chi(t) / V_\chi(t)$ is the concentration of ethanol in the compartment. The compartment subscripts are $\mathscr{V}$ for the Vascular, $\mathscr{T}$ for the peripheral tissue, and $\mathscr{L}$ for the Liver parenchyma.

Each edge of the graph is labeled with a name if it clearly corresponds to a particular anatomical structure, and is labeled with the ethanol mass flow [$M_\mathrm{X}(t)$ variable] and the volume flow [$R_\mathrm{X}(t)$ variable] that occur along that edge. The edges are directed, which indicates the positive flux direction. In addition, $C_\mathrm{X}(t) \doteq M_\mathrm{X}(t) / R_\mathrm{X}(t)$ is the concentration of ethanol in the edge. The edge subscripts are A for aorta, P for peripheral artery, VC for vena cava, PV for portal vein, HA for hepatic artery, HV for hepatic vein, and Cap for peripheral capillary bed.

The mass flows $M_{\mathrm{Gut}}(t)$ and $M_{\mathrm{Infuse}}(t)$ are the external in puts to the system and represent the flow of ethanol from the gut and from a venous infusion, respectively. The mass flow $M_{\mathrm{Metab}}(t)$ is the ethanol sink created by liver metabolism of ethanol.

There are three kinds of vertices in the graph. The first type is the compartment where the entering and exiting edges form the right-hand side of a differential equation for the state variable. The second type are vertices where only one edge enters (no symbol) that obey Kirchhoff's current law (KCL) and divide the input fluxes (ethanol mass and volume) among the edges that exit. The F_X constants indicate the fraction of the input that exits on each of

the exiting edges. The subscripts are L for fraction of the cardiac output directed to the liver and PV for the fraction of the liver-directed cardiac output that is directed through the gut and the portal vein. The third type are vertices where only one edge exits (Σ symbol) that obey KCL and sum the input fluxes (ethanol mass and volume) in order to determine the fluxes (ethanol mass and volume) on the edge that exits. Since the second and third type of vertices both obey KCL, they are really the same.

IV. Three-State PBPK3 Model

The three-state PBPK3 model is shown in Fig. 1 and is a generalization of the two-state PBPK2 model developed at the Indiana Alcohol Research Center, Indiana University School of Medicine. The state equations can be read directly from Fig. 1 and are

$$\frac{d\mu_{\mathscr{L}}}{dt}(t) = M_{\mathrm{HA},\mathscr{L}}(t) + M_{\mathrm{PV},\mathscr{L}}(t) - M_{\mathscr{L},\mathrm{HV}}(t) - M_{\mathrm{Metab}}(t) \tag{4}$$

$$\frac{d\mu_{\mathscr{T}}}{dt}(t) = M_{\mathrm{P},\mathscr{T}}(t) - M_{\mathscr{T},\mathrm{P}}(t) \tag{5}$$

$$\begin{aligned}\frac{d\mu_{\mathscr{V}}}{dt}(t) &= M_{\mathrm{HA}}(t) - M_{\mathrm{HA},\mathscr{L}}(t) + M^{(2)}_{\mathrm{PV}}(t) - M_{\mathrm{PV},\mathscr{L}}(t) + M_{\mathscr{L}\mathrm{HA}}(t) + M_{\mathrm{P}}(t) + M_{\mathscr{T},\mathrm{P}}(t) - M_{\mathrm{P},\mathscr{T}}(t) - M_{\mathrm{A}}(t) + M_{\mathrm{Infuse}}(t) \\ &= -M_{\mathrm{HA}\mathscr{L}}(t) - M_{\mathrm{PV},\mathscr{L}}(t) + M_{\mathscr{L},\mathrm{HV}}(t) + M_{\mathscr{T},\mathrm{P}}(t) - M_{\mathrm{P},\mathscr{T}}(t) + M_{\mathrm{Infuse}}(t) + M_{\mathrm{Gut}}(t).\end{aligned} \tag{6}$$

Therefore, it remains only to provide equations in terms of $\mu_{\chi}(t)$ for $M_{\mathrm{Metab}}(t)$, $M_{\mathrm{HA},\mathscr{L}}(t)$, $M_{\mathrm{PV},\mathscr{L}}(t)$, $M_{\mathscr{L},\mathrm{HV}}(t)$, $M_{\mathscr{T},\mathrm{P}}(t)$, and $M_{\mathrm{P},\mathscr{T}}(t)$, since $M_{\mathrm{Infuse}}(t)$ and $M_{\mathrm{Gut}}(t)$ are external inputs.[3] Since conservation of ethanol mass is enforced, the time derivative of the sum $\mu_{\mathscr{L}}(t) + \mu_{\mathscr{T}}(t) + \mu_{\mathscr{V}}(t)$ equals the inputs $[M_{\mathrm{Infuse}}(t) + M_{\mathrm{Gut}}(t)]$ minus the outputs $[M_{\mathrm{Metab}}(t)]$ which provides an alternative method to derive (6).

Equations for the six unknown mass fluxes can be derived in terms of the three state variables. The mass flux from the liver parenchyma out of the system, which is denoted by $M_{\mathrm{Metab}}(t)$, is directly determined by MM kinetics, that is,

$$M_{\mathrm{Metab}}(t) = V_{\mathscr{L}} V_{\max} \frac{\mu_{\mathscr{L}}(t)/V_{\mathscr{L}}}{K_m + \mu_{\mathscr{L}}(t)/V_{\mathscr{L}}}. \tag{7}$$

The remaining five unknown mass fluxes can be derived following the general principles that result in (2) and (3). Four of the fluxes, $M_{\mathrm{P},\mathscr{T}}(t)$ (20), $M_{\mathscr{T},\mathrm{P}}(t)$ (21), $M_{\mathrm{HA},\mathscr{L}}(t)$ (22), and $M_{\mathrm{PV},\mathscr{L}}(t)$ (23) follow directly from the principles and the results are listed in the Appendix.

The determination of the mass flux from the liver parenchyma to the hepatic vein, which is denoted by $M_{\mathscr{L},\mathrm{HV}}(t)$, is more complicated because it requires the solution of a nonlinear equation in order to determine the ethanol concentration in the hepatic vein. The solution of this nonlinear equation, which allows the model to be expressed as a system of three nonlinear ordinary differential equations without additional constraints, is one of the contributions of this paper. Define

$$\alpha(t) = \frac{1}{R_{\mathrm{A}} F_{\mathrm{L}}} \left(M_{\mathrm{HA}}(t) - M_{\mathrm{HA},\mathscr{L}}(t) + M^{(2)}_{\mathrm{PV}}(t) - M_{\mathrm{PV},\mathscr{L}}(t) \right) \tag{8}$$

[2]Simulink is a trademark of The MathWorks, http://www.mathworks. com/.

$$\gamma(t) = \frac{\mu_{\mathscr{L}}(t)}{V_{\mathscr{L}}} \tag{9}$$

where formulas for $M_{\mathrm{HA}}(t)$ (24), $M_{\mathrm{HA},\mathscr{L}}(t)$ (22), $M_{\mathrm{PV}}^{(2)}(t)$ (25), and $M_{\mathrm{PV},\mathscr{L}}(t)$ (23) are listed in the Appendix. Then, it can be shown that

$$C_{\mathrm{HV}}(t) = \alpha(t) + k_{\mathscr{L},\mathrm{HV}}\, r\left(\gamma(t) - C_{\mathrm{HV}}(t)\right)$$

which implies that

$$\frac{1}{k_{\mathscr{L},\mathrm{HV}}}\left[C_{\mathrm{HV}}(t) - \alpha(t)\right] = r\left(\gamma(t) - C_{\mathrm{HV}}(t)\right). \tag{10}$$

Note that $C_{\mathrm{HV}}(t)$ occurs twice in (10), which is a nonlinear equation, and so (10) must be solved for $C_{\mathrm{HV}}(t)$. Consider the case $k_{\mathscr{L},\mathrm{HV}} > 0$. By plotting the left- and right-hand sides of (10) with respect to $C_{\mathrm{HV}}(t)$, it can be seen that there is always an intersection between the two curves, so that a solution always exists, and that the intersection, which defines the solution for $C_{\mathrm{HV}}(t)$, obeys the switching equation

$$C_{\mathrm{HA}}(t) = \begin{cases} \frac{1}{1+k_{\mathscr{L}\mathrm{HV}}}\left(\alpha(t) + k_{\mathscr{L},\mathrm{HV}}\gamma(t)\right), & \alpha(t) < \gamma(t) \\ \alpha(t), & \alpha(t) > \gamma(t) \end{cases}. \tag{11}$$

For $k_{\mathscr{L},\mathrm{HV}} = 0$, the solution is always $C_{\mathrm{HV}}(t) = \alpha(t)$. For $k_{\mathscr{L},\mathrm{HV}} < 0$, the situation is more complicated, since zero, one, or two solutions can exist. However, this case is not important since $k_{\mathscr{L},\mathrm{HV}} < 0$ implies transport of ethanol up rather than down its concentration gradient. The final mass flux needed to evaluate (4)–(6) is $M_{\mathscr{L},\mathrm{HV}}(t)$, which is given by (26) in the Appendix.

In summary, the total model is composed of the three nonlinear ordinary differential equations for the state variables [(4)–(6)]; the eight mass flux equations needed to evaluate (4)–(6), which are the external inputs $M_{\mathrm{Gut}}(t)$ and $M_{\mathrm{Infuse}}(t)$ and the six internal variables $M_{\mathrm{Metab}}(t)$, $M_{\mathrm{P},\mathscr{T}}(t)$, $M_{\mathscr{T},\mathrm{P}}(t)$, $M_{\mathrm{HA},\mathscr{L}}(t)$, $M_{\mathrm{PV},\mathscr{L}}(t)$, and $M_{\mathscr{L},\mathrm{HV}}(t)$ [(7), (20)–(23), and (26), respectively]; $M_{\mathrm{PV}}^{(2)}(t)$ and $M_{\mathrm{HA}}(t)$ [(25) and (24)] needed to evaluate $\alpha(t)$ (8), $\gamma(t)$ (9), and $C_{\mathrm{HV}}(t)$ (11).

V. Two-State PBPK2 Model

The liver compartment volume $V_{\mathscr{L}}$ is difficult to determine noninvasively and inexpensively in a test subject. Therefore, a model that does not require a value for $V_{\mathscr{L}}$ is attractive. In addition, a goal of this paper is to demonstrate the flexibility of the PBPK modeling viewpoint. Therefore, consider a second model which is the block diagram shown in Fig. 1 with A replaced by A'. The second model has only two states and does not require a value for $V_{\mathscr{L}}$. This model is exactly the PBPK2 model developed and routinely implemented at the Indiana Alcohol Research Center, Indiana University School of Medicine.

The analysis of the PBPK2 model is very similar to the analysis of the PBPK3 model presented in Section IV. The major difference is the definition of the liver ethanol concentration that is required in order to compute the ethanol elimination mass flow from

Michaelis-Menten kinetics. The concentration of ethanol in the liver is taken as the concentration of ethanol entering the liver, which is not a compartment, which is

$$\begin{aligned} C_{\mathscr{L}}(t) &= \frac{M_{\mathrm{HA}}(t)+M_{\mathrm{PV}}^{(2)}(t)}{R_{\mathrm{HA}}+R_{\mathrm{PV}}^{(2)}} \\ &= \frac{\mu_{\mathscr{V}}(t)}{V_{\mathscr{V}}}+\frac{M_{\mathrm{Gut}}(t)}{R_{\mathrm{A}}F_{\mathrm{L}}}. \end{aligned} \tag{12}$$

The term $M_{\mathrm{Metab}}(t)$ is direct from MM kinetics based on the $C_{\mathscr{L}}(t)$ computed before, where $M_{\max}$ ([mass]/[time]) is a new parameter that plays the role of $V_{\mathscr{L}}V_{\max}$ resulting in the equation

$$M_{\mathrm{Metab}}(t) = M_{\max}\frac{C_{\mathscr{L}}(t)}{K_m+C_{\mathscr{L}}(t)}. \tag{13}$$

In summary, the resulting equations are the two state equations,

$$\frac{d\mu_{\mathscr{T}}}{dt}(t) = M_{\mathrm{P},\mathscr{T}}(t) - M_{\mathscr{T},\mathrm{P}}(t) \tag{14}$$

$$\frac{d\mu_{\mathscr{V}}}{dt}(t) = -\frac{\mu_{\mathscr{V}}(t)}{V_{\mathscr{V}}}R_{\mathrm{A}}F_{\mathrm{L}}+M_{\mathscr{T},\mathrm{P}}(t)-M_{\mathrm{P},\mathscr{T}}(t)+r\left[\frac{\mu_{\mathscr{V}}(t)}{V_{\mathscr{V}}}R_{\mathrm{A}}F_{\mathrm{L}}+M_{\mathrm{Gut}}(t)-M_{\mathrm{Metab}}(t)\right]+M_{\mathrm{Infuse}}(t) \tag{15}$$

the expressions for $C_{\mathscr{L}}(t)$ (12), $M_{\mathrm{Metab}}(t)$ (13), $M_{\mathrm{P},\mathscr{T}}(t)$ (20), and $M_{\mathscr{T},\mathrm{P}}(t)$ (21); and the two external inputs $M_{\mathrm{Gut}}(t)$ and $M_{\mathrm{Infuse}}(t)$.

The anomalous behavior of the PBPK2 model is the fact that the mass flow of ethanol being degraded may potentially be greater than the mass flow of ethanol entering the liver. Since the liver in the PBPK2 model does not store ethanol, this is nonphysical. The lower limit on the liver ethanol concentration can be computed as follows. The mass flux of ethanol entering the liver, the mass flux of ethanol being metabolized in the liver, and the ethanol concentration in the liver are

$$M_{\mathrm{enter}} = M_{\mathrm{HA}}(t)+M_{\mathrm{PV}}^{(2)}(t), \tag{16}$$

$$M_{\mathrm{Metab}}(t) = M_{\max}\frac{C_{\mathscr{L}}(t)}{K_m+C_{\mathscr{L}}(t)}, \tag{17}$$

$$C_{\mathscr{L}}(t) = \frac{M_{\mathrm{enter}}(t)}{R_{\mathrm{HA}}+R_{\mathrm{PV}}^{(2)}}, \tag{18}$$

respectively. The fundamental requirement is $M_{\mathrm{Metab}}(t) \le M_{\mathrm{enter}}(t)$ which implies

$$M_{\max}/\left(R_{\mathrm{HA}}+R_{\mathrm{PV}}^{(2)}\right) - K_m \le C_{\mathscr{L}}(t). \tag{19}$$

For a worst-case human subject, $M_{\max}$ = 300 mg/min,[4] $R_{\mathrm{HA}}+R_{\mathrm{PV}}^{(2)}$=11.7 dL/min, and K_m = 10 mg/dL, so the lower limit on $C_{\mathscr{L}}(t)$ is 15.64 mg/dL, which is substantially below the level at which a human is intoxicated or at which data are recorded [23], [45]. For that reason, this characteristic of the PBPK2 model was not observed nor it was a concern, although a ramp function has been included at the hepatic vein in order to guarantee that the mass flow of

ethanol in the hepatic vein is nonnegative. Note that the PBPK3 model does not have a similar nonphysical region.

VI. Numerical Results

The parameters needed for a two-state (i.e., PBPK2) model were computed for a female subject first by the morphometric method and then subsequently by the optimization scheme detailed in [30]. The results are R_A = 42.3071 dL/min, $V_{\mathcal{T}}$ =14.69 L, $V_{\mathcal{V}}$ =11.846 L, $M_{\max}=V_{\mathcal{L}}\,V_{\max}$=147.03 mg/min, and $k_{X,Y}$ = 0.2951 (for all values of x and y). Consistent with values determined by other investigators developing models [40], [46]–[48], F_{L} = 0.26, F_{PV} = 0.75, and K_m = 10 mg/dL per [19]. The resultant BrAC from an infusion profile computed based upon these parameters is discussed in the third paragraph of this section and is displayed in Fig. 2.

For the three-state (i.e., PBPK3) model, the liver volume $V_{\mathcal{L}}$ is estimated [18, p. 1554] as proportional to lean body mass with a constant of 0.033 (0.024) L/kg for women (men) and the lean body mass is estimated [49] as the total body water divided by 0.725 L/kg. The result is $V_{\mathcal{L}}$ =12.863 dL. The other parameters of the PBPK3 model are the same as the parameters of the PBPK2 model except that the volume of the peripheral tissue compartment ($V_{\mathcal{T}}$) is reduced by the volume of the liver.

The following example, concerning an intravenous ethanol infusion, demonstrates and contrasts the PBPK2 and PBPK3 models. The goal of the experiment is to prescribe ascending and descending slopes of BrAC after a preliminary experiment is utilized to determine parameters. The goal is met in the first 40 min, but BrAC was tracked for another 60 min after the infusion pumps were turned off [Fig. 2(a)] in order to provide further modeling validation data. The experimental BrAC measurements and the simulation trajectories of vascular and peripheral state variables from both models are shown in Fig. 2(b) along with the time course of liver ethanol concentration from the three-state PBPK3 model. A major feature of Fig. 2(b) is that the computed two-state PBPK2 vascular ethanol concentration curve is an excellent fit to all of the experimental BrAC data, as would be expected since the parameters of the PBPK2 model for this subject were determined in a separate experiment on this subject. Further, the trajectories of the PBPK2 and PBPK3 models match rather accurately on the upslope but differ on the downslope potentially due to the fact that the peripheral tissue acts as a reservoir for ethanol which, in the PBPK3 model, must be transported twice (to the vascular, and then, to the liver compartments) before it can be metabolized, while in the PBPK2 model, it only needs to be transported once (to the vascular compartment). As would be expected with ethanol infusion, there is no first-pass elevation in liver ethanol concentration and no first-pass metabolism. In fact, the liver concentration is always less than the BrAC. While it is beyond the scope of this paper to develop a method for identifying the parameters of a three-state (i.e., PBPK3) model analogous to the method of [30], it should be possible to develop such a method when data that reflects the concentrations in the liver compartment can be measured on human subjects and the model is available in a standard mathematical format, as is achieved in this paper, rather than as a software package. Identification of the liver volume by such a method could

[3]Although $M_{\mathrm{Gut}}(t)$ = 0 in the example of this paper, $M_{\mathrm{Gut}}(t)$ is retained in the model because it is the path for oral ethanol, the dominant mode of ethanol self-administration, to enter the model. Let $M_{\mathrm{Oral}}(t)$ be the ethanol mass flow at the mouth. In [43] and [44], a phenomenological linear time-invariant model relating $M_{\mathrm{Oral}}(t)$ and $M_{\mathrm{Gut}}(t)$ is used, $M_{\mathrm{Gut}}(t) = M_{\mathrm{Oral}}(t) * h_{\mathrm{Gut}}(t)$, where * denotes convolution and $h_{\mathrm{Gut}}(t)$ is a critically damped second-order system that integrates to 1, $h_{\mathrm{Gut}}(t) = \beta^2\, t \exp(-\beta t)u(t)$, where the integration condition is necessary and sufficient to achieve $\int_{-\infty}^{+\infty} M_{\mathrm{Oral}}(t)\,dt = \int_{-\infty}^{+\infty} M_{\mathrm{Gut}}(t)\,dt$ so that all ethanol is eventually absorbed.

be compared to liver volumes obtained by computed tomographic scanning of the subjects as an additional validation procedure.

VII. Discussion

This paper studies the PBPK2 model of ethanol, developed at the Alcohol Research Center, Indiana University School of Medicine. This model and its applications are focused on representing and prescribing the exposure of an individual human subject. The application dictated modeling parsimony, minimizing complexity of the model since parameters are determined from morphometric measurements of an individual. The PBPK2 model has been validated in a variety of ways, with an example provided in Section VI. Face validity follows from its demonstrated utility in numerous successful ethanol challenge studies in humans using the clamping paradigm [6], [7], [12]–[14], [18]–[23], [25]–[27], [29], [30]. Extensions of the original clamping paradigm to applications that were not contemplated when the model was developed (e.g., slopes) also validate the model through utility. Application of model parameter optimization methods, based on experimental data from an individual rather than on morphometric transformation [30], with demonstration of subsequent improvement in prescriptive accuracy, also support the validity of the underlying model. Genetic analysis of parameters derived from parameter identification in sibling-pair paradigms, showing higher estimates of heritability in the $V_{\max}$ parameter as compared to conventional methods of estimating ethanol elimination rates in the same subjects [29], also connotes model validity. As one measure of confidence in the model, the Indiana University School of Medicine Institutional Review Board (IRB) has approved the use of the PBPK2 model for prescribing brain ethanol exposures in the functional magnetic resonance imaging (fMRI) environment, where measurements of BrAC cannot be obtained during the infusion, at levels of exposure that would be unsafe if oral administration was employed. Finally, the model was used successfully to achieve ethanol clamping in another species, rats, with no change to the model architecture [24], [28]

The contributions of this paper are described at the end of Section I. The description of models of this type as systems of ordinary differential equations enables the use of modern system identification, filtering, and control system design methodologies, and work in this direction is underway [43], [44]. The methods used in this paper allow for structured exploration and possible conversion of some of the phemenological aspects of ethanol models to more physiologic model representations. For example, the combined MM elimination pathway models as described herein could possibly be expanded to explore contributions of the dominant enzyme systems responsible for alcohol metabolism: cytosolic alcohol dehydrogenase, cytochrome P-4502E1, and mitochodrial aldehyde dehydrogenase [5], [22]. Validation of such a model with multiple elimination pathways would be challenging: 1) higher ethanol concentrations would be required in order to activate enzyme systems other than alcohol dehydrogenase and aldehyde dehydrogenase and 2) it would probably be necessary to convert the model to an experimental animal, such as pigs, in which instrumentation of the hepatic artery, portal vein, and hepatic vein is possible. Developments such as these could then allow for exploration of the relative contributions of these systems to alcohol metabolism in conditions of clinical interest, such as precirrhotic alcohol dependence and periodic alcohol abuse as well as cirrhosis. In this paper, the PBPK2 model is derived as an approximation to the PBPK3 model. It would be enlightening if standard mathematical methods, such as singular perturbations, could be used to achieve this reduction in the order of the system of differential equations from 3 to 2, and this is under investigation. In addition to correcting the anomalous behavior of the PBPK2 model, the PBPK3 model allows future study of more naturalistic oral challenge paradigms, and ethanol concentrations in the liver, which can be substantially higher than in other organs because of first-pass exposure to orally ingested ethanol.

One implied obligation of this study is eventual validation of the PBPK3 model. One route to this future work is translational research. Because the validity of the PBPK2 model has been demonstrated in rats, that species offers the opportunity to instrument the animals with portal vein and hepatic vein catheters to gather data for validation of the PBPK3 model, both in health and after experimental liver injury. Allometric scaling would permit the assessment of human liver injury without the need for expensive and potentially hazardous invasive instrumentation. The cost, additional modeling complexity, is minimal since good estimates of liver volume in healthy human subjects can be obtained from morphometric measures, and individual estimates of liver volume, in subjects with liver dysfunction, can be obtained with noninvasive computed tomography. Alternatively, advances in compound localization and concentration determination via imaging (e.g., magnetic resonance spectroscopy), may allow direct noninvasive measurement of ethanol concentrations relevant to the liver compartment of the PBPK3 model.

Modeling advances, such as those described in this paper, are central to determining mathematical models (including the parameter values) for individual subjects that will better predict their unique response to ethanol. Using such models, it is already possible to design dose trajectories for individuals such that all individuals have the same, possibly very complex, brain exposure to ethanol, even in environments, such as fMRI, where the experimental BrAC cannot be monitored. Extension of the PBPK2 model to the PBPK3 formulation offers the ability to employ the technology in other novel applications to human ethanol research, such as interpretation of data from the implantable ethanol biosensor, and may open the way for eventually assessing liver injury in alcoholic patients.

Acknowledgments

This work was supported by the National Institute of Health (NIH) under Grant N01AA23102, Grant P60 AA07611-16-17, and under NIAA R01 AA12555-05.

APPENDIX

MASS FLUX EQUATIONS FOR SECTION IV

$$M_{\mathrm{P},\mathscr{T}}(t) = k_{\mathrm{P},\mathscr{T}} R_{\mathrm{A}} (1 - F_{\mathrm{L}}) r \left(\frac{\mu_{\mathscr{V}}(t)}{V_{\mathscr{V}}} - \frac{\mu_{\mathscr{T}}(t)}{V_{\mathscr{T}}} \right) \tag{20}$$

$$M_{\mathscr{T},\mathrm{P}}(t) = k_{\mathscr{T},\mathrm{P}} R_{\mathrm{A}} (1 - F_{\mathrm{L}}) r \left(\frac{\mu_{\mathscr{T}}(t)}{V_{\mathscr{T}}} - \frac{\mu_{\mathscr{V}}(t)}{V_{\mathscr{V}}} \right) \tag{21}$$

$$M_{\mathrm{HA},\mathscr{L}}(t) = k_{\mathrm{HA},\mathscr{L}} R_{\mathrm{A}} F_{\mathrm{L}} (1 - F_{\mathrm{PV}}) r \left(\frac{\mu_{\mathscr{V}}(t)}{V_{\mathscr{V}}} - \frac{\mu_{\mathscr{L}}(t)}{V_{\mathscr{L}}} \right) \tag{22}$$

$$M_{\mathrm{PV},\mathscr{L}}(t) = k_{\mathrm{PV},\mathscr{L}} R_{\mathrm{A}} F_{\mathrm{L}} F_{\mathrm{PV}} r \left(\frac{\mu_{\mathscr{V}}(t)}{V_{\mathscr{V}}} + \frac{M_{\mathrm{Gut}}(t)}{R_{\mathrm{A}} F_{\mathrm{L}} F_{\mathrm{PV}}} - \frac{\mu_{\mathscr{L}}(t)}{V_{\mathscr{L}}} \right) \tag{23}$$

$$M_{\mathrm{HA}}(t) = R_{\mathrm{A}} F_{\mathrm{L}} (1 - F_{\mathrm{PV}}) \frac{\mu_{\mathscr{V}}(t)}{V_{\mathscr{V}}} \tag{24}$$

$$M_{\mathrm{PV}}^{(2)}(t) = \frac{\mu_{\mathscr{V}}(t)}{V_{\mathscr{V}}} R_{\mathrm{A}} F_{\mathrm{L}} F_{\mathrm{PV}} + M_{\mathrm{Gut}}(t) \tag{25}$$

$$M_{\mathscr{L},\mathrm{HV}}(t) = k_{\mathscr{L},\mathrm{HV}} R_{\mathrm{A}} F_{\mathrm{L}} r\left(\frac{\mu_{\mathscr{L}}(t)}{V_{\mathscr{L}}} - C_{\mathrm{HV}}(t)\right). \tag{26}$$

Biographies

Martin H. Plawecki (S'96) received the B.S. degree in electrical engineering, the Ph.D. degree in biomedical engineering, both from Purdue University, West Lafayette, IN, in 1999 and 2005, respectively, and the M.D. degree from Indiana University School of Medicine, IN, in 2007.

He joined the Indiana Medical Scientist Training Program, a joint M.D.-Ph.D.program between the Weldon School of Biomedical Engineering, Purdue University and the Indiana University School of Medicine. He is currently a Resident in the Psychiatry Program, Indiana University School of Medicine, Indianapolis.

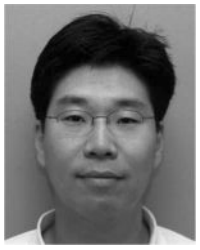

Jae-Joon Han (S'06) received the B.S. degree in electronic engineering from Yonsei University, Seoul, South Korea, in 1997, the M.S. degree in electrical and computer engineering from the University of Southern California, Los Angeles, in 2001, and the Ph.D. degree in electrical and computer engineering from Purdue University, West Lafayette, IN, in 2006.

From 2001 to 2006, he was a Teaching Assistant, and then, a Research Assistant in the School of Electrical and Computer Engineering, Purdue University, where he was also a Postdoctoral Fellow pursuing research in biomedical modeling and stochastic inference. In September 2007, he joined Samsung Advanced Institute of Technology as an R&D Staff Member.

Peter C. Doerschuk (S'79–M'86–SM'03) received the B.S., M.S., and Ph.D. degrees in electrical engineering from Massachusetts Institute of Technology (MIT), Cambridge, and the M.D. degree from Harvard Medical School, Boston, MA.

He did postgraduate training at Brigham and Womens' Hospital. From January 1988 to August 1990, he was a Postdoctoral Fellow at the Laboratory for Information and Decision Systems (MIT). In July 2006, after 16 years with the Faculty of Electrical and Computer Engineering, Purdue University, he joined the Faculty of Biomedical Engineering and Electrical and Computer Engineering, Cornell University, Ithaca, NY.

Vijay A. Ramchandani received the B.S. degree in pharmaceutical sciences from Bombay University, Mumbai, India, in 1990, and the Ph.D. degree in pharmaceutical sciences from Virginia Commonwealth University, Richmond, in 1996.

From 1996 to 2002, he was at the Indiana Alcohol Research Center at Indiana University School of Medicine, first as a Research Associate, and then, as an Assistant Scientist and a Part-Time Assistant Professor. Since January 2003, he has been a Staff Scientist in the Intramural Research Program of the National Institute on Alcohol Abuse and Alcoholism, National Institutes of Health, Bethesda, MD.

Sean J. O'Connor received the B.S. and M.S. in electrical engineering from Cornell University, Ithaca, NY, in 1965 and 1967, respectively, and the M.D. degree from the University of Connecticut School of Medicine, Farmington, CT, in 1978. He completed Psychiatric Residency also at the University of Connecticut, Connecticut School of Medicine, in 1982.

He is currently a Faculty member in psychiatry at Indiana University School of Medicine, Indianapolis, and in biomedical engineering at Purdue University, West Lafayette, IN. His

current research interests in clude genetic determinants of the human brain's adaptive response to alcohol. He directs three laboratories where subjective perceptions, neuropsychologic tests, eye movements, and EEG are used to characterize the ways people who are more vulnerable to future alcoholism respond differently to alcohol when compared to controls.

REFERENCES

[1]. Alcohol and Coronary Heart Disease. National Institute on Alcohol Abuse and Alcoholism; 1999. Alcohol Alert No. 45-1999

[2]. Schuckit MA, Smith TL, Danko GP, Kramer J, Godinez J, Bucholz KK, Nurnberger JI Jr. Hesselbrock V. Prospective evaluation of the four DSM-IV criteria for alcohol abuse in a large population. Amer. J. Psychiatry. Feb; 2005 162(2):350–360. [PubMed: 15677601]

[3]. Paykin HD. A. alcohol dependence and abuse diagnoses: Concurrent validity in a nationally respresentative sample. Alcohol.: Clinical Exp. Res. Jan; 1999 23(1):144–150. [PubMed: 10029216]

[4]. Beers, MH.; Berkow, R. The Merck Manual of Diagnosis and Therapy. 17th ed. Merck Research Lab; Whitehouse Station, NJ: 1999.

[5]. Gentry RT. Effect of food on the pharmacokinetics of alcohol absorption. Alcohol.: Clinical Exp. Res. Apr; 2000 24(4):403–404. [PubMed: 10798565]

[6]. Ramchandani VA, O'Connor S, Neumark Y, Zimmermann US, Morzorati SL, de Wit H. The alcohol clamp: Applications, challenges, and new directions—An RSA 2004 symposium summary. Alcohol.: Clinical Exp. Res. Jan; 2006 30(1):155–164. [PubMed: 16433744]

[7]. Ramchandani VA, Li TK, Plawecki MH, O'Connor S. Mimicking the breath alcohol exposure following oral alcohol administration using IV ethanol infusions in healthy volunteers: Characterization of pharmacokinetic variability. submitted for publication.

[8]. Khanna JM, Le AD, Kalant H, Chau A, Shah G. Effect of lipid solubility on the development of chronic cross-tolerance between ethanol and different alcohols and barbiturates. Pharmacol. Biochem. Behav. 1997; 57(1/2):101–110. [PubMed: 9164559]

[9]. Jones AW, Hahn RG, Stalberg HP. Pharmacokinetics of ethanol in plasma and whole blood: Estimation of total body water by the dilution principle. Eur. J. Clin. Pharmacol. 1992; 42:445–448. [PubMed: 1516610]

[10]. Kaneko T, Wang P-Y, Sato A. Partition coefficients of some acetate esters and alcohols in water, blood, olive oil, and rat tissues. Occup. Environ. Med. 1994; 51:68–72. [PubMed: 8124468]

[11]. Pastino GM, Sultatos LG, Flynn EJ. Development and application of a physiologically based pharmacokinetic model for ethanol in the mouse. Alcohol Alcohol. 1996; 31(4):365–374. [PubMed: 8879283]

[12]. Blekher T, Ramchandani VA, Flury L, Foroud T, Kareken D, Yee RD, Li T-K, O'Connor S. Saccadic eye movements are associated with a family history of alcoholism at baseline and after exposure to alcohol. Alcohol Clin. Exp. Res. 2002; 26(10):1568–1573. [PubMed: 12394291]

[13]. Blekher T, Beard JD, O'Connor S, Orr WE, Ramchandani VA, Miller K, Yee RD, Li TK. Response of saccadic eye movements to alcohol in African American and non-Hispanic white college students. Alcohol.: Clinical Exp. Res. Feb; 2002 26(2):232–238. [PubMed: 11964563]

[14]. Morzorati SL, Ramchandani VA, Flury L, Li TK, O'Connor S. Self-reported subjective perception of intoxication reflects family history of alcoholism when breath alcohol levels are constant. Alcohol.: Clinical Exp. Res. Aug; 2002 26(8):1299–1306. [PubMed: 12198408]

[15]. Erblich J, Earleywine M. Children of alcoholics exhibit attenuated cognitive impairment during an ethanol challenge. Alcohol.: Clinical Exp. Res. Mar; 1999 23(3):476–482. [PubMed: 10195821]

[16]. Schuckit M, Smith T, Pierson J, Danko G, Beltran IA. Relationships among the level of response to alcohol and the number of alcoholic relatives in predicting alcohol-related outcomes. Alcohol.: Clinical Exp. Res. Aug; 2006 30(8):1308–1314. [PubMed: 16899033]

[17]. Gibb KA, Yee AS, Johnston CC, Martin SD, Nowak RM. Accuracy and usefulness of a breath alcohol analyzer. Ann. Emergency Med. Jul; 1984 13(7):516–520.

[18]. Kwo PY, Ramchandani VA, O'Connor S, Amann D, Carr LG, Sandrasegaran K, Kopecky KK, Li T-K. Gender differences in alcohol metabolism: Relationship to liver volume and effect of adjusting for body mass. Gastroenterology. 1998; 115(6):1552–1557. [PubMed: 9834284]

[19]. Ramchandani VA, Bolane J, Li TK, O'Connor S. A Physiologically based pharmacokinetic (PBPK) model for alcohol facilitates rapid BrAC clamping. Alcohol Clin. Exp. Res. 1999; 23

[20]. Ramchandani VA, O'Connor S, Blekher T, Kareken D, Nurnberger MSJ Jr. Li TK. A preliminary study of acute responses to clamped alcohol concentration and family history of alcoholism. Alcohol Clin. Exp. Res. Aug; 1999 23(8):1320–1330. [PubMed: 10470974]

[21]. O'Connor S, Ramchandani VA, Li T-K. PBPK modeling as a basis for achieving a steady BrAC of 60±5 mg% within ten minutes. Alcohol Clin. Exp. Res. 2000; 24:426–427. [PubMed: 10798577]

[22]. Li TK, Yin SJ, Crabb DW, O'Connor S, Ramchandani VA. Genetic and environmental influences on alcohol metabolism in humans. Alcohol Clin. Exp. Res. 2001; 25(1):136–144. [PubMed: 11198709]

[23]. Ramchandani VA, Kwo PY, Li T-K. Influence of food and food composition on alcohol elimination rates in healthy men and women. J. Clin. Pharmacol. 2001; 41:1345–1350. [PubMed: 11762562]

[24]. Morzorati SL, Ramchandani VA, Li TK, O'Connor S. A method to achieve and maintain steady state blood alcohol levels in rats using a physiologically based pharmacokinetic model. Alcohol. 2002; 28:189–195. [PubMed: 12551760]

[25]. Ramchandani VA, Flury L, Morzorati SL, Kareken D, Blekher T, Foroud T, Li TK, O'Connor S. Recent drinking history: Association with family history of alcoholism and the acute response to alcohol during a 60 mg% clamp. Alcohol Clin. Exp. Res. Nov; 2002 63(6):734–744.

[26]. Subramanian MG, Heil SH, Kruger ML, Collins KL, Buck PO, Zawacki T, Abbey A, Sokol RJ, Diamond MP. A three-stage alcohol clamp procedure in human subjects. Alcohol Clin. Exp. Res. 2002; 26:1479–1483. [PubMed: 12394280]

[27]. Neumark YD, Friedlander Y, Durst R, Leitersdorf E, Jaffe D, Ramchandani VA, O'Connor S, Carr LG, Li T-K. Alcohol dehydrogenase polymorphisms influence alcohol-elimination rates in a male Jewish population. Alcohol Clin. Exp. Res. 2004; 28:10–14. [PubMed: 14745297]

[28]. Morzorati SL, Stewart RB. Development of acute tolerance during steady-state arterial alcohol concentrations: A study of auditory event-related potentials in rats. Alcohol Clin. Exp. Res. Mar; 2005 29(3):347–352. [PubMed: 15770109]

[29]. Famchandani VA, Flury L, Plawecki MH, Foroud T, O'Connor S. Heritability of alcohol elimination kinetics in sibling pairs. Alcoholism: Clinical Exp. Res. (Supplement). May.2005 29(5):84a. [28th Annual Meeting of the Research Society on Alcoholism, June 25-30, 2005, Santa Barbara, CA, Poster P567].

[30]. Plawecki MH, DeCarlo RA, Ramchandani VA, O'Connor S. Improved transformation of morphometric measurements for a priori parameter estimation in a Physiologically based pharmacokinetic model of ethanol. Biomed. Signal Process. Control. Apr; 2007 2(2):97–110. [PubMed: 18379641]

[31]. Widmark, EMP. Principles and Applications of Mediocolegal Alcohol Determination. Biomedical Publication; Davis: 1981. [authorized English translation of the 1932 German edition entitled Die theoretischen Grundlagen und die praktische Verwendbarkeit der gerichtlich-medizinischen Alkoholbestimmung with permision of Urban & Schwarzenberg]

[32]. Whitmire D, Cornelius L, Whitmire P. Monte Carlo simulation of an ethanol pharmacokinetic model. Alcohol Clin. Exp. Res. 2002; 26(10):1494–1493. [PubMed: 12394282]

[33]. Pastino GM, Asgharian B, Roberts K, Medinsky MA, Bond JA. A comparison of physiologically based pharmacokinetic model predictions and experimental data for inhaled ethanol in male and female B6C3F_1 mice, F344 rats, and humans. Toxicol. Appl. Pharmacol. Jul; 1997 145(1):147–157. [PubMed: 9221833]

[34]. Pastino GM, Conolly RB. Application of a physiologically based pharmacokinetic model to estimate the bioavailability of ethanol in male rats: Distinction between gastric and hepatic pathways of metabolic clearance. Toxicol. Sci. 2000; 55:256–265. [PubMed: 10828256]

[35]. Sultatos LG, Pastino GM, Rosenfeld CA, Flynn EJ. Incorporation of the genetic control of alcohol dehydrogenase into a physiologically based pharmacokinetic model for ethanol in humans. Toxicol. Sci. 2004; 78:20–31. [PubMed: 14718645]

[36]. Gentry RT. Determinants and analysis of blood alcohol concentration after social drinking. Alcohol Clin. Exp. Res. 2000; 24(4):399. [PubMed: 10798563]

[37]. Stryer, L. Biochemistry. 4th ed.. Freeman; New York: 1999.

[38]. Guyton, AC.; Hall, JE. Textbook of Medical Physiology. 9th ed.. Saunders; Philadelphia, PA: 1996.

[39]. Weiss, TF. Cellular Biophysics: Transport. Vol. vol.1. MIT Press; Cambridge, MA: 1996.

[40]. Rheingold JL, Lindstrom RE, Wilkinson PK. A new blood-flow pharmacokinetic model for ethanol. J. Pharmacokinet. Biopharm. 1981; 9:261–278. [PubMed: 7288592]

[41]. Matsumoto H, Fukui Y. Pharmacokinetics of ethanol: A review of the methodology. Addict. Biol. 2002; (7):5–14. [PubMed: 11900618]

[42]. Boleda MP, Julia P, Moreno A, Pares X. Role of extrahepatic alcohol dehydrogenase in rat ethanol metabolism. Arch. Biochem. Biophys. 1989; 274:74–81. [PubMed: 2774584]

[43]. Plawecki, MH. Ph.D. dissertation. Weldon School Biomed. Eng., Purdue Univ.; West Lafayette, IN: May. 2005 A Physiologically based pharmacokinetic (PBPK) model for ethanol: Mathematical foundations, parameter identification, and other applications.

[44]. Han, J-J. Ph.D. dissertation. School Elect. Comput. Eng., Purdue Univ.; West Lafayette, IN: Aug. 2006 Statistical signal processing and pattern recognition for an implantable ethanol biosensor.

[45]. Brown RP, Delp MD, Lindstedt SL, Rhomberg LR, Beliles RP. Physiological parameter values for physiologically based pharmacokinetic models. Toxicol. Ind. Health. 1997; 13:407–484. [PubMed: 9249929]

[46]. Andersen ME, Clewell HJ III, Gargas ML, Smith FA, Reitz RH. Physiologically based pharmacokinetics and the risk assessment process for methylene chloride. Toxicol. Appl. Pharmacol. 1987; 87:185–205. [PubMed: 3824380]

[47]. Shoaf S. Pharmacokinetics of intravenous alcohol: Two compartment, dual Michaelis-Menten elimination. Alcohol Clin. Exp. Res. 2000; 24(4):424–425. [PubMed: 10798576]

[48]. Baraona E, Abittan CS, Dohmen K, Moretti M, Pozzato G, Chayes ZW, Schaefer C, Lieber C. Gender differences in pharmacokinetics of alcohol. Alcohol.: Clin. Exp. Res. Apr; 2001 25(4): 502–507. [PubMed: 11329488]

[49]. Watson PE, Watson ID, Batt RD. Total body water volumes for adult males and females estimated from simple anthropometric measurements. Am. J. Clin. Nutr. 1980; 33:27–29. [PubMed: 6986753]

[50]. Wilkinson PK, Sedman AJ, Sakmar E, Earhart RH, Weidler DJ, Wagner J. Blood ethanol concentrations during and following constant-rate intravenous infusions of alcohol. Clin. Pharmacol. Ther. Feb; 1976 19(2):213–223. [PubMed: 1261158]

[51]. Wilkinson PK, Sedman AJ, Sakmar E, Lin YJ, Wagner JG. Fasting and nonfasting blood ethanol concentrations following repeated oral administration of ethanol to one adult male subject. J. Pharmacokinet. Biopharm. 1977; 5:41–52. [PubMed: 845791]

[52]. Rangno RE, Kreeft JH, Sitar DS. Ethanol “dose-dependent” elimination: Michaelis-Menten V classical kinetic analysis. Br. J. Clin. Pharmacol. 1981; 12:667–673. [PubMed: 7332732]

[53]. Mumenthaler MS, Taylor JL, Yesavage JA. Ethanol pharmacokinetics in white women: Nonlinear model fitting versus zero-order elimination analyses. Alcohol Clin. Exp. Res. 2000; 24(4):1353–1362. [PubMed: 11003200]

[54]. Levitt MD, Levitt DG. Use of a two-compartment model to predict ethanol metabolism. Alcohol Clin. Exp. Res. 2000; 24(4):409–410. [PubMed: 10798568]

[55]. Norberg A, Gabrielsson J, Jones AW, Hahn RG. Within- and between-subject variations in pharmacokinetic parameters of ethanol by analysis of breath, venous blood, and urine. Br. J. Clin. Pharmacol. 2000; (49):399–408. [PubMed: 10792196]

[56]. Pastino GM, Flynn EJ, Sultatos LG. Genetic polymorphisms in ethanol metabolism: Issues and goals for physiologically based pharmacokinetic modeling. Drug Chem. Toxicol. Feb; 2000 23(1):179–201. [PubMed: 10711397]

[57]. Norberg A, Sandhagen B, Bratteby L-E, Gabrielsson J, Jones AW, Fan H, Hahn RG. Do ethanol and deuterium oxide distribute into the same water space in healthy volunteers? Alcohol Clin. Exp. Res. 2001; 25(10):1423–1430. [PubMed: 11696661]

[58]. Umulis DM, Gürmen NM, Singh P, Fogler HS. A physiologically based model for ethanol and acetaldehyde metabolism in human beings. Alcohol. 2005; 335:3–12. [PubMed: 15922132]

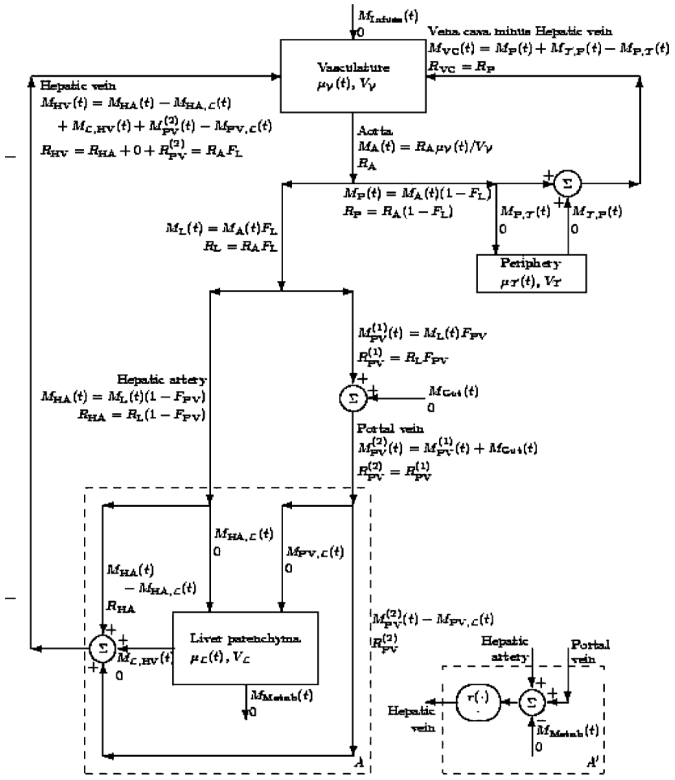

Fig. 1.

Block diagrams for PBPK-like models. A complete three-compartment model is shown. In addition, an alternative model for the liver (replace A by A') is shown that reduces the model to a two-compartment model. In submodel A', the oval containing $r(\cdot)$ and $\cdot$ means to pass the mass flux through a unit ramp function in order to guarantee that it is positive and to pass the volume flux unaltered, i.e., through the identity map. The labels for the edges are left justified unless the edge is to the right of the label in which case the labels are right justified.

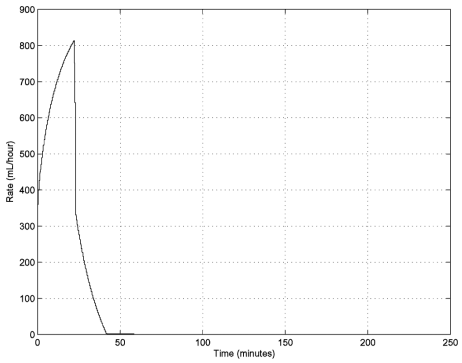

(a)

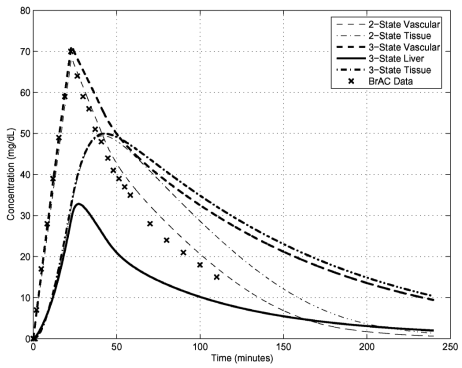

(b)

Fig. 2.

Intravenous input of a 6% ethanol solution [Panel (a)] and experimental BrAC measurements and PBPK2 and PBPK3 state-variable trajectories after conversion to concentrations [Panel (b)] for the “slopes” IV input. The parameters for the models come from previous measurements on the same human subject for which the BrAC data were recorded.

TABLE I

Summary of Selected Other Mathematical Models for Ethanol Pharmacokinetics in Chronological Order of Publication

Author	N ‡	Type	Elimination	Input	Subjects
Widmark [31]	1	PK	0^{th}	Oral	Human
Wilkinson [50]	1	PK	MM	IV	Human
Wilkinson [51]	1	PK	MM	Oral	Human
Rangno [52]	2	PK	MM	Oral, IV	Human
Jones [9]	2	PK‡	MM	IV	Human
Pastino [11]	7	PBPK	Dual MM	IP	Rat
Pastino [33]	6	PBPK	MM	Inhaled	Human *, Mouse, Rat
Shoaf [47]	2	PK	Dual MM	IV	Human *
Mumenthaler [53]	2, 1	PK	1^{st} & MM	Oral	Human†
Levitt [54]	2	PBPK	MM	Oral+IV	Human *
Norberg [55]	2	PK	MM	IV	Human
Pastino [34]	7	PBPK	Dual MM	Oral	Rat *
Pastino [56]	8	PBPK	Dual MM	Oral	Human *
Norbert [57]	2, 1	PK	Dual MM	IV	Human
Whitmire [32]	5	PBPK	Dual MM	GL	Dog
Sultatos [35]	8	PBPK	MM	IV	Human *
Umulis§ [58]	5	PBPK	MM	Oral	Human *

Author	Compartments of PBPK model
Pastino [11]	lung, rapidly perfused, slowly perfused, fat, brain, liver
Pastino [33]	lung, rapidly perfused, slowly perfused, fat, brain, liver
Levitt [54]	TBW, liver
Pastino [34]	lung, rapidly perfused, slowly perfused, fat, brain, liver, stomach
Pastino [56]	lung, rapidly perfused, slowly perfused, fat, brain, liver, GI-1, GI-2
Whitmire [32]	TBW, stomach mucosa, stomach lumen, duodenal villi, duodenal lumen
Sultatos [35]	lung, rapidly perfused, slowly perfused, fat, brain, liver, stomach, small intestine
Umulis [58]	stomach, GI, central, muscle, liver

The abbreviations are PK: pharmacokinetic, PBPK: physiologically-based pharmacokinetic, MM: Michaelis-Menten, 0^{th} : 0^{th} order, 1^{st}: 1^{st} order, IV: intravenous infusion, IP: intraperitoneal injection, GL: gastric lavage, TBW: total body water, and GI: gastrointestinal.

[ǂ]Number of compartments.

[*]Previously published data.

[†]Female subjects.

[§]Umulis [58] describes the kinetics of both ethanol and acetaldehyde.

[ǂ]Jones [9] describes whole blood and plasma kinetics but there is no overall model and it is difficult to select PK versus PBPK category.

IEEE Trans Biomed Eng. Author manuscript; available in PMC 2012 September 19.